Colloids and Surfaces B: Biointerfaces 81 (2010) 50–57

Contents lists available at ScienceDirect

Colloids and Surfaces B: Biointerfaces

journal homepage: www.elsevier.com/locate/colsurfb

Milk whey proteins and xanthan gum interactions in solution and at the air–water interface: A rheokinetic study

Adrián A. Perez[a], Cecilio Carrera Sánchez[b], Juan M. Rodríguez Patino[b], Amelia C. Rubiolo[a], Liliana G. Santiago[a,*]

[a] Grupo de Biocoloides, Instituto de Tecnología de Alimentos, Facultad de Ingeniería Química, Universidad Nacional del Litoral, Santa Fe, Argentina
[b] Departamento de Ingeniería Química, Facultad de Química, Universidad de Sevilla, Sevilla, Spain

ARTICLE INFO

Article history:
Received 11 February 2010
Received in revised form 23 June 2010
Accepted 24 June 2010
Available online 9 August 2010

Keywords:
Whey protein concentrate
β-Lactoglobulin
Xanthan gum
Protein–polysaccharide interactions
Adsorption kinetics
Interfacial rheology
Air–water interface

ABSTRACT

In this contribution, we present experimental information about the effect of xanthan gum (XG) on the adsorption behaviour of two milk whey protein samples (MWP), β-lactoglobulin (β-LG) and whey protein concentrate (WPC), at the air–water interface. The MWP concentration studied corresponded to the protein bulk concentration which is able to saturate the air–water interface (1.0 wt%). Temperature, pH and ionic strength of aqueous systems were kept constant at 20 °C, pH 7 and 0.05 M, respectively, while the XG bulk concentration varied in the range 0.00–0.25 wt%. Biopolymer interactions in solution were analyzed by extrinsic fluorescence spectroscopy using 1-anilino-8-naphtalene sulphonic acid (ANS) as a protein fluorescence probe. Interfacial biopolymer interactions were evaluated by dynamic tensiometry and surface dilatational rheology. Adsorption behaviour was discussed from a rheokinetic point of view in terms of molecular diffusion, penetration and conformational rearrangement of adsorbed protein residues at the air–water interface. Differences in the interaction magnitude, both in solution and at the interface vicinity, and in the adsorption rheokinetic parameters were observed in MWP/XG mixed systems depending on the protein type (β-LG or WPC) and biopolymer relative concentration. β-LG adsorption in XG presence could be promoted by mechanisms based on biopolymer segregative interactions and thermodynamic incompatibility in the interface vicinity, resulting in better surface and viscoelastic properties. The same mechanism could be responsible of WPC interfacial adsorption in the presence of XG. The interfacial functionality of WPC was improved by the synergistic interactions with XG, although WPC chemical complexity might complicate the elucidation of molecular events that govern adsorption dynamics of WPC/XG mixed systems at the air–water interface.

1. Introduction

Surface dynamic properties of emulsifiers at fluid interfaces are of a great importance for colloidal food formulations [1,2]. Protein adsorption rate at the air–water and oil–water interfaces is considered to play a determinant role in the formation and stabilization of foams and emulsions [3–5]. Interfacial adsorption behaviour can be described by different mechanisms [6–9]: (i) protein transport from the bulk phase to the subsurface layer immediately adjacent to the fluid interface by diffusion, (ii) protein penetration and unfolding at the interface, and (iii) rearrangement of the adsorbed protein segments, a slow mechanism caused by reorganization of the hydrophobic amino acids previously adsorbed at the interface. In addition to lower the interfacial tension, protein can form a viscoelastic film at the interface via non-covalent intermolecular interactions and covalent disulphide cross-linking, which is a key factor for the stability of colloidal food dispersions [10–12].

On the other hand, although much is known about protein surface properties in model studies, predictions of protein interfacial adsorption behaviour in real food systems are needed to rationally design foams and emulsions [2,13,14]. Product formulation engineering should contemplate factors such as those that influence the conformational stability of proteins (pH, ionic strength, temperature, and shear), the purification and production processes (membrane separation methods, heat processing, spray-drying technology) and the protein intermolecular interactions with other ingredients of the food matrix [15–20]. Thus, the proper control of physical or physico-chemical principles could improve the quality and performance of food dispersed systems through an adequate correlation between the interfacial nanostructure and the engineering processes [15,21–23].

Milk whey proteins (MWP) are known to alter their adsorption behaviour at fluid interfaces responding to both different aqueous environmental conditions [24–26] and the presence of several

* Corresponding author. Tel.: +54 342 4571252x2602.
E-mail address: lsanti@fiq.unl.edu.ar (L.G. Santiago).

0927-7765/$ – see front matter © 2010 Elsevier B.V. All rights reserved.
doi:10.1016/j.colsurfb.2010.06.021

food additives such as lipids [2,27], sugars [28,29], electrolytes [5], polypeptides [30], polysaccharides [2], etc. However, in order to establish the efficiency of proteins as emulsifiers in food dispersed systems, studies on the interactions between MWP and other ingredients should be performed in a systematic and quantitative way.

The study of protein adsorption dynamics related to the presence of polysaccharides (PS) in model systems (purified proteins and PS) has recently received greater attention [1,2]. Protein–polysaccharide interactions can be used to control protein adsorption at fluid interfaces [31,32] and to modulate rheological properties of adsorbed films [33,34]. However, due to the chemical complexity and variability of the biopolymer sources that are normally used in food dispersions, fundamental studies on real systems (involving industrial available proteins and PS) are required. Thus, acquired knowledge would have a direct practical interest for the food industry.

In this paper, we examine the impact of the interactions between MWP and xanthan gum (XG), a non-surface-active polysaccharide commonly used as a thickening agent [35], on the protein adsorption and rheokinetic behaviour at the air–water interface, at neutral pH and low ionic strength. In the present work, β-lactoglobulin (β-LG) and whey protein concentrate (WPC) were chosen because MWP utilization is increasing in the formulation of dairy aerated foods mainly due to their high nutritional value [36,37]. Nevertheless, differences in aggregation state [38–40] and molecular composition, which derive from the cheese making process [41,42] and the separation methods [43], limit the application of WPC as functional ingredient. Recently, the influence of non-surface PS, such as λ-carrageenan (λ-C) and sodium alginate (SA), on the interfacial dynamics and surface rheological properties of WPC adsorbed films at the air–water interface has been determined [44,45]. The main results of this research reveal the importance of biopolymer interaction mechanisms at the air–water interface (complexation and/or segregation) in the control of formation and rheological characteristics of WPC adsorbed films as a function of polysaccharide chemical nature, biopolymer relative concentration and molecular dynamics of protein–polysaccharide interactions in solution [46]. In this context, the use of XG as a stabilizing agent could balance and promote better functions of MWP through biopolymer interactions.

2. Materials and methods

2.1. Biopolymer samples

Whey protein isolate (WPI), a protein sample with a very high content of β-LG (protein 92 ± 2%, β-lactoglobulin > 95%, α-lactalbumin < 5%, fat maximum 0.2%) was supplied by Danisco Ingredients (Brabrand, Denmark). As WPI sample contains over 95% β-LG, and the mineral and lipid contents are very low, it would be reasonable to describe this protein sample as "β-LG". WPC, industrially produced, was kindly provided by Arla Food (Porteña, Cordoba, Argentina) and it was used without purification. This product is a spray-dried WPC obtained from sweet whey after rennet casein precipitation by low-temperature ultrafiltration. Its composition was: protein 76.81% ($N \times 6.38$); moisture 4.52%; lactose (maximum) 9.00%; fat 2.01%; ash 2.05%; and others 5.61%. Ions present in WPC powder were quantified by atomic-flame emission spectroscopy of ashed sample and the values were (wt%): Ca^{2+} 0.31; Na^{+} 0.2%; Mg^{2+} 0.1%; Cl^{-} 0.05%, K^{+} 0.6%, and phosphorous 0.3%. The nitrogen solubility index (NSI) was determined by standard methods (AACC [47]) with a milk protein factor, $N \times 6.38$. The WPC sample had a NSI = 94.26% at pH 7. The determination of denatured protein percentage [48] revealed the presence of 84% of native and 16% of denatured protein in the WPC sample. Further WPC physico-chemical analysis, such as size exclusion HPLC (SE-HPLC), and differential scanning calorimetry (DSC) has been outlined in [46]. This characterization revealed the existence of protein aggregates of variable size (178–523 kDa) and that β-LG is the majority protein fraction in the WPC sample. Xanthan gum (XG) obtained from a natural strain of *Xanthomonas campestris* was kindly supplied by Cargill (Buenos Aires, Argentina). The XG molecular weight was 4000 kDa. XG powder has the following composition (data supplied by Cargill): carbohydrate 73.0%; pyruvic acid ≥1.5%; moisture 15.0%; and ash 9.0% (Na^{+} 2900 mg/100 g and K^{+} 320 mg/100 g, Ca^{+2} 50 mg/100 g, and Mg^{+2} 70 mg/100 g).

2.2. Aqueous systems preparation

Milk whey proteins (β-LG and WPC) and XG samples were dissolved in Milli-Q ultrapure water at room temperature, and pH and ionic strength were adjusted to 7 and 0.05 M, respectively, with a commercial buffer solution called trizma ($(CH_2OH)_3$-C-NH_2/$(CH_2OH)_3$-C-NH_3Cl) (Sigma, USA). The absence of surface-active contaminants in the aqueous buffered solution was checked by interfacial tension measurement before the preparation of dispersions. No aqueous solutions with a surface tension other than that accepted in the literature (72–73 mN/m at 20 °C) were used. A stock XG dispersion (0.50 wt%) was stirred for at least 1 h at 80 °C to ensure complete dispersion and it was subsequently left overnight at 4–5 °C to hydrate appropriately. The presence of surface-active impurities in the stock XG dispersion was checked by the interfacial tension measurement and removed by repetitive suctions. After six suctions (the last one after 24 h of preparation) the sample had a surface pressure of ≈4 mN/m, which confirmed that most surface-active impurities in XG dispersion had been removed by suction. This purified XG dispersion was used in this study. MWP concentration was kept constant at 1.0 wt% in all experiments and XG concentration varied in the range 0.00–0.25 wt%. MWP/XG aqueous systems were obtained by mixing the appropriate volume of each double concentrated biopolymer solution up to the final required concentration. It should be noted that there was a very slight difference in the ionic strength of aqueous systems due to ions contained in the biopolymer samples.

2.3. Extrinsic fluorescence measurement

The MWP–XG interactions in solution were analyzed by extrinsic fluorescence spectroscopy using 1-anilino-8-naphtalene sulphonic acid (ANS, Fluka Chemie AG, Switzerland) as a protein fluorescence probe [46,49]. Serial dilutions in trizma buffer were obtained from MWP and MWP/XG aqueous systems. Dilutions were prepared at pH 7 up to a final concentration of 0.01–0.50 mg/ml. Ten microliters of ANS (8 mM) were added to 2 ml of each dilution and the fluorescence intensity (FI) was measured at 350 nm (excitation) and 470 nm (emission). The initial slope of the FI (arbitrary unit, a.u.) versus protein concentration (mg/ml) plot was calculated by linear regression analysis, and was used as an index of protein surface hydrophobicity (S_0). Each S_0 measure was obtained in triplicate.

2.4. Dynamic surface properties measurement

The MWP–XG interactions at the air–water interface were evaluated by means of dynamic tensiometry and surface dilatational rheology. The MWP concentration (1.0 wt%) used in this study resulted in the maximum surface pressure value at equilibrium, associated with the saturation of an adsorbed monolayer at the air–water interface [44,50]. MWP and MWP/XG aqueous systems

were stirred for 30 min at room temperature (20–23 °C) before the interfacial measurements were performed. Dynamic surface pressure (π) and surface dilatational measurements for MWP and MWP/XG adsorbed films at the air–water interface were performed with an automatic pendant drop tensiometer (TRACKER, IT Concept, Longessaine, France) as already described [51]. The method involved a periodic automated-controlled, sinusoidal interfacial compression and expansion performed by decreasing and increasing the drop volume at the desired amplitude ($\Delta A/A$) and angular frequency (ω). The surface dilatational modulus (E) derived from the change in interfacial tension (σ) resulting from a small change in surface area may be described by Eq. (1) [52]:

$$E = \frac{d\sigma}{dA/A} = -\left(\frac{d\pi}{d\ln A}\right) = |E|e^{i\phi} = E_d + iE_v \quad (1)$$

where $|E| = (|E_d|^2 + |E_v|^2)^{1/2}$.

Surface dilatational modulus (E), as a measure of the total material resistance to dilatational deformation (elastic + viscous), is a complex quantity and it is composed of real and imaginary parts. The real part of the dilatational modulus (or storage component) is the dilatational elasticity, $E_d = |E|\cos\phi$. The imaginary part of the dilatational modulus (or loss component) is the surface dilatational viscosity, $E_v = |E|\sin\phi$. The phase angle (ϕ) between stress and strain is a measure of the relative film viscoelasticity. For a perfectly elastic material stress and strain are in phase ($\phi = 0$) and the imaginary term is zero. In the case of a perfectly viscous material, $\phi = 90°$ and the real part is zero.

Interfacial experiments were carried out at 20 ± 0.3 °C. The temperature of the experimental system was maintained constant by circulating water from a thermostat. MWP and MWP/XG solutions were placed in the syringe and subsequently in a compartment, and they were allowed to stand for 30 min to reach the desired constant temperature. Then a drop was delivered and allowed to stand for 10,800 s to achieve protein adsorption at the air–water interface. Surface rheological parameters (E, E_d, E_v and ϕ) were measured as a function of adsorption time (θ), at 10% of deformation amplitude ($\Delta A/A$) and at 10 s of period of oscillation (T). Sinusoidal oscillation for surface dilatational measurement was made with five oscillation cycles followed by a time of 50 cycles without any oscillation up to the time required to complete adsorption. Measurements were made at least twice. The average standard accuracy of the surface pressure was roughly 0.1 mN/m. The reproducibility of the results was better than 0.5% and 5.0% for surface pressure and surface dilatational properties, respectively.

2.5. Rheokinetic approach

Protein adsorption at the air–water interface can be monitored by measuring changes in interfacial pressure (π). The rate of change of surface concentration (Γ) can be expressed as [6]:

$$\frac{d\Gamma}{d\theta} = \left(\frac{d\Gamma}{d\pi}\right)\left(\frac{d\pi}{d\theta}\right) \quad (2)$$

If ($d\Gamma/d\pi$) is constant, $d\pi/d\theta$ can be used to evaluate the protein adsorption rate. During the first step, at relatively low pressures when diffusion is the rate determining step, a modified form of the Ward and Tordai equation [53] can be used to correlate the change in the interfacial pressure with time (Eq. (3)).

$$\pi = 2C_0KT\left(\frac{D\theta}{3.14}\right)^{1/2} \quad (3)$$

where C_0 is the concentration in the bulk phase, K is the Boltzmann constant, T is the absolute temperature, and D is the protein diffusion coefficient. If the protein diffusion toward the interface controls the adsorption process, a plot of π against $\theta^{1/2}$ will then be linear [6,54].

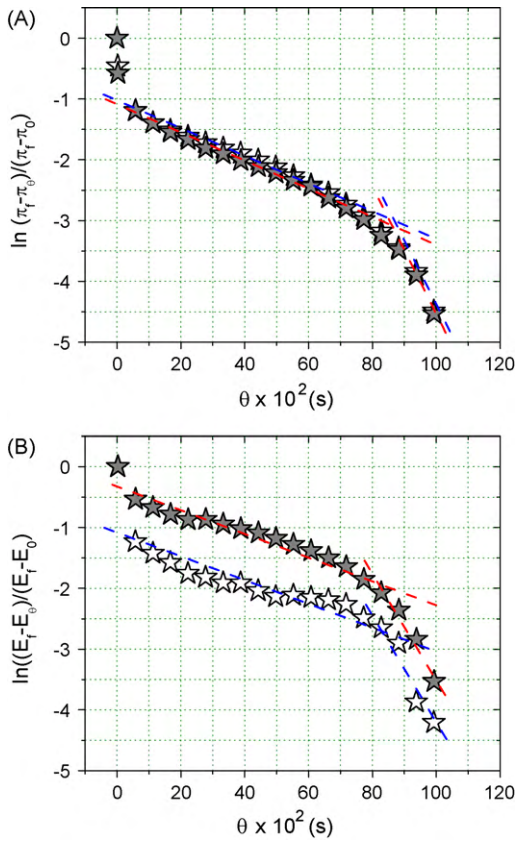

Fig. 1. Rheokinetic model applied to the adsorption mechanisms for (⋆) β-LG and (☆) WPC at the air–water interface. Dashed lines indicate the experimental data set subject to linear regression model in order to obtain the first-order constants for penetration and molecular rearrangement of protein adsorbed segments at the air–water interface: (A) using Eq. (4): $\ln(\pi_f - \pi_\theta)/(\pi_f - \pi_0) = -k_i\theta$ and (B) using Eq. (5): $\ln(E_f - E_\theta)/(E_f - E_0) = -k_i'\theta$. MWP concentration 1.00 wt%, temperature 20 °C, pH 7, and I 0.05 M.

Furthermore, to monitor molecular penetration and configurational rearrangement of adsorbed protein segments at the interface, two different approaches can be used. Firstly, the rate of these adsorption processes can be analyzed by a first-order equation [7,8],

$$\frac{\ln(\pi_f - \pi_\theta)}{(\pi_f - \pi_0)} = -k_i\theta \quad (4)$$

where π_f, π_0, and π_θ are the interfacial pressures at the final adsorption time of each step, at the initial time, θ_0, and at any time θ, respectively, and k_i is a first-order rate constant. In practice, a plot of Eq. (4) usually yields in two or more linear regions. The initial slope is taken to correspond to a first-order rate constant of molecular penetration (k_P), while the second slope is taken to correspond to a first-order rate constant of configurational rearrangement (k_R), occurring among a more or less constant number of adsorbed segments. As an example, the application of Eq. (4) to MWP adsorption at the air–water interface is given in Fig. 1a.

It is well known that the time-dependent surface pressure follows the same trend as the protein surface concentration [6,55] indicating that π and E depend on surface coverage, which is expected to increase with θ. Due to this similarity, we propose a first-order kinetic equation (Eq. (5)) similar to Eq. (4) to evaluate the molecular penetration and the configurational rearrangement

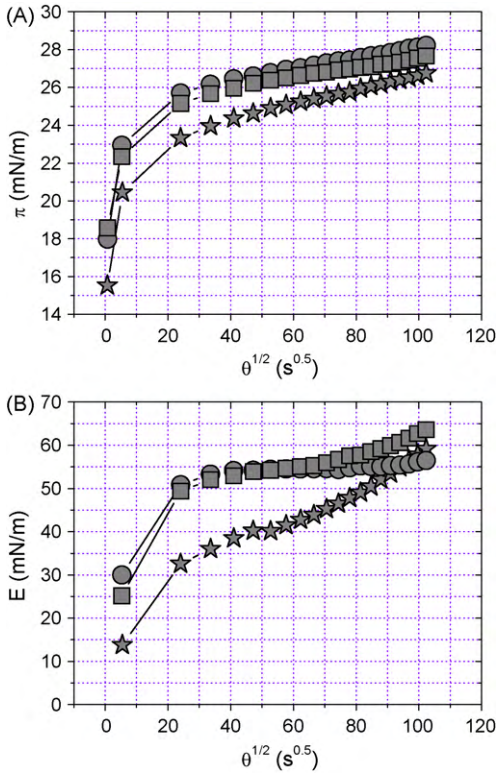

Fig. 2. Time dependence of surface pressure, π (A) and surface dilatational modulus, E (B) for (⋆) β-LG adsorbed films at the air–water interface as a function of XG bulk concentration (0.00–0.25 wt%). β-LG:XG symbols: (■) 1.00:0.25 wt% and (●) 1.00:0.10 wt%. β-LG concentration 1.00 wt%, temperature 20 °C, pH 7, and I 0.05 M.

of adsorbed protein residues at the air–water interface,

$$\frac{\ln(E_f - E_\theta)}{(E_f - E_0)} = -k_i'\theta \quad (5)$$

where E_f, E_0, and E_θ are the surface dilatational modulus at the final adsorption time of each step, at the initial time, θ_0, and at any time θ, respectively, and k_i' are the first-order rate constants of protein penetration and further rearrangement at the interface. This proposal can be viewed in Fig. 1b for MWP adsorption at the air–water interface.

3. Results and discussion

3.1. Impact of β-LG/XG interaction on protein surface properties

3.1.1. Surface pressure

Dynamic surface pressure (π) for β-LG adsorbed films at the air–water interface as a function of XG bulk concentration (0.00–0.25 wt%) is plotted in Fig. 2 a. In the absence of XG, an increment in surface pressure with time (θ) can be seen, behaviour that could be associated with β-LG interfacial adsorption [9,55,56]. On the other hand, the magnitude of this phenomenon was influenced by XG concentration in solution. XG caused an increment in the surface pressure of the β-LG adsorbed film (Fig. 2a). Similar results were obtained by Baeza et al. who showed that the increase in surface pressure of the β-LG/XG mixed system could indicate a strong synergism between these biopolymers [31]. XG could enhance the β-LG adsorption mainly through a thermodynamic incompatibility phenomenon in the interface vicinity depending on its concentration in solution. Under these conditions, the existence of segregative mechanisms between both biopolymers at the air–water interface could lead to changes in surface pressure of protein adsorbed film due to modification

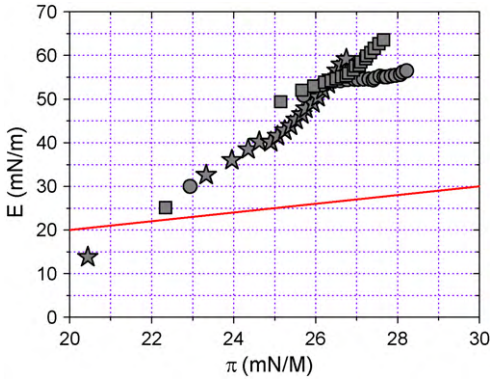

Fig. 3. Surface dilatational modulus (E) as a function of surface pressure (π) for (⋆) β-LG adsorbed films at the air–water interface and XG bulk concentration (0.00–0.25 wt%). β-LG:XG symbols: (■) 1.00:0.25 wt% and (●) 1.00:0.10 wt%. β-LG concentration 1.00 wt%, temperature 20 °C, pH 7, and I 0.05 M.

both of protein thermodynamic activity in the presence of the polysaccharide [57] and the biopolymer relative concentration in solution [44]. Moreover, segregative mechanism of proteins [58–60], protein/surface-active polysaccharides [31,33,61], and protein/non-surface-active polysaccharides [31,33,44,45] in aqueous systems and at the air–water interface are all well documented in the literature.

3.1.2. Surface dilatational properties

From a rheological point of view, over the adsorption period studied, it can be observed that the viscoelastic behaviour of MWP (β-LG and WPC) and MWP/XG (β-LG/XG and WPC/XG) adsorbed films at the air–water interface was essentially elastic (especially at long-term adsorption), and can be analyzed by: (i) E and E_d values were similar, and (ii) values of both E_v and ϕ were low (data not shown here).

Dynamic dilatational modulus (E) for β-LG adsorbed films at the air–water interface as a function of XG bulk concentration (0.00–0.25 wt%) is plotted in Fig. 2b. The E values for β-LG and β-LG/XG adsorbed films increased with θ. This phenomenon could also be related with β-LG interfacial adsorption [9,55,56], but more specifically could be interpreted in terms of an increased mechanical resistance of the adsorbed films due to an increment in protein–protein interactions at the air–water interface [62,63]. At short adsorption time, XG caused an increment in E values for the β-LG adsorbed film, while at long-term adsorption these values were similar or higher than pure β-LG depending on the biopolymer relative concentration in solution. In general, results for β-LG/XG systems are consistent with the existence of higher protein–protein interactions, which could be favoured by the thermodynamic incompatibility between β-LG and XG in the interface vicinity [33].

On the other hand, if the magnitude of the surface dilatational modulus is a consequence of the adsorbed protein amount at the air–water interface, every E data should be normalized in a single master curve of E versus π. In the case of globular proteins, E increases with π suggesting an increase in macromolecular interactions among adsorbed protein segments [62,63]. The E–π master curves for β-LG/XG adsorbed films at 0.00–0.25 wt% XG bulk concentration are shown in Fig. 3. The slopes of E–π plots were higher than one (represented by the solid line in Fig. 3); therefore, a non-ideal behaviour was confirmed suggesting the existence of higher protein–protein interactions at the interface [64]. Moreover, E–π plots for β-LG/XG adsorbed films were not normalized in a unique curve, indicating that the interfacial structuration (packing and/or condensation) was affected by the presence of XG and the

Table 1
Influence of XG concentration (0.00–0.25 wt%) on the MWP surface hydrophobicity (S_0). S_0 values are presented as mean ± SD. MWP concentration 1.00 wt%, temperature 20 °C, pH 7, and *I* 0.05 M.

System	MWP:XG (wt%)	S_0
β-LG	1.00:0.00	181 ± 2
β-LG:0.10XG	1.00:0.10	183 ± 1
β-LG:0.25XG	1.00:0.25	188 ± 2
WPC	1.00:0.00	265 ± 3
WPC:0.10XG	1.00:0.10	246 ± 4
WPC:0.25XG	1.00:0.25	256 ± 2

biopolymer relative concentration in solution. In the presence of XG, differences in β-LG interfacial packing could be a consequence of different rates of molecular penetration and configurational rearrangement of the adsorbed residues, as reflected by the values of surface dilatational modulus for β-LG/XG absorbed films (Fig. 2b). This hypothesis will be discussed from a rheokinetic point of view.

3.2. Impact of β-LG/XG interaction on protein adsorption rheokinetics

3.2.1. Protein diffusion

According to Ward and Tordai [53] the protein adsorption kinetics at short time can be deduced from the π–$\theta^{1/2}$ curves, being the slope of these plots the diffusion rate constant (k_{diff}). At the MWP (β-LG and WPC) bulk concentration used in this study (1.0 wt%), the protein diffusion step (both with and without XG) was too fast (with $\pi > 10$ mN/m) to be detected by the experimental method used in this work (as deduced from π values for β-LG and WPC adsorbed films in Figs. 2a and 5a, respectively). The same behaviour was observed for the molecular diffusion of soy globulins (7S and 11S) at 1.0 wt% protein concentration [65]. Thus, the initial slope of the π–$\theta^{1/2}$ curve at the beginning of the adsorption (at 0.5 s) can be considered a measure of the apparent diffusion rate (k^a_{diff}). As it can be observed in Fig. 4 a, the increment in XG concentration caused an increased β-LG k^a_{diff}. These results might suggest that molecular dynamics in solution of β-LG/XG mixed systems could play a decisive role in the β-LG diffusion step toward the air–water interface.

The magnitude of the intermolecular interactions between β-LG and XG could depend on biopolymer relative concentration in aqueous subphase. In order to evaluate the incidence of β-LG–XG interactions in solution on the molecular diffusion behaviour toward the interface, exposed hydrophobicity of β-LG/XG mixed systems was determined [44]. Table 1 shows the effect of XG bulk concentration (0.00–0.25 wt%) on β-LG surface hydrophobicity (S_0). It can be noticed that XG caused a increment in β-LG S_0 values which could be related with a higher exposure of the β-LG hydrophobic *patches* in the presence of XG confirming the highest protein diffusion toward the interface (Fig. 4a) and β-LG greater ability to form an adsorbed film (as deduced from π values for β-LG and β-LG/XG systems in Fig. 2a). As mentioned above, this phenomenon could be associated with the existence of a thermodynamic incompatibility mechanism between β-LG and XG in the vicinity of the air–water interface [44,57]. Moreover, this evidence indicated that the greater the surface hydrophobicity of the β-LG/XG mixed systems, the greater the β-LG diffusion rate to the interface, which confirms results from previous studies [44–46].

3.2.2. Protein penetration and rearrangement

At higher adsorption time, after the very short period controlled by diffusion, an energy barrier for β-LG adsorption appears which

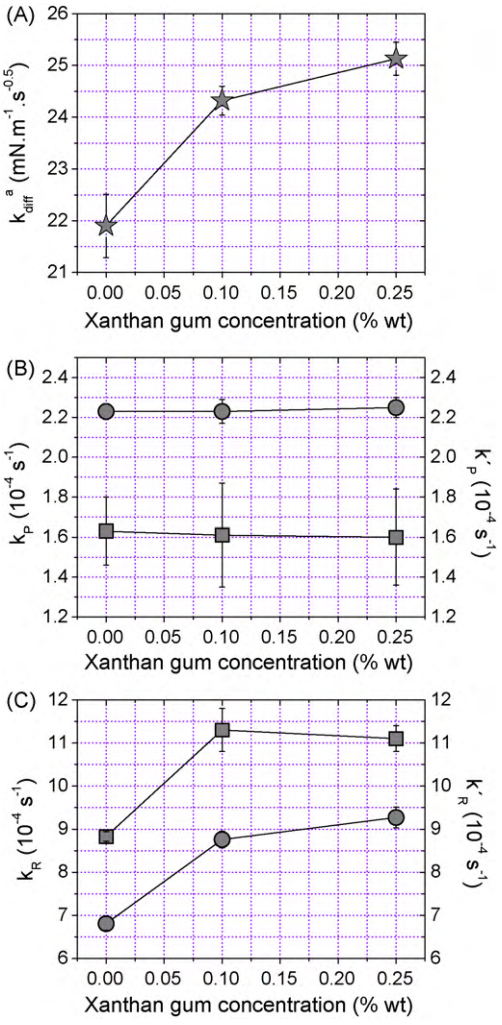

Fig. 4. Effect of XG bulk concentration (0.00–0.25 wt%) on: (A) apparent rate of diffusion to the interface (k^a_{diff}), (B) penetration rate constant obtained from Eq. (4), k_P, and Eq. (5), k'_P, and (C) configurational rearrangement rate constant obtained from Eq. (4), k_R and Eq. (5), k'_R for β-LG/XG mixed systems. β-LG concentration 1.00 wt%, temperature 20 °C, pH 7, and *I* 0.05 M.

can be attributed to adsorption, penetration, unfolding, and rearrangements of the protein at the air–water interface [7,8].

Fig. 4b and c shows the application of Eqs. (4) and (5) to β-LG/XG mixed systems. It was noticed that the proposed rheokinetic model was adequate to describe the long-term adsorption mechanisms of the biopolymer mixed systems ($R > 0.970$ in all cases). In addition, both approach (Eqs. (4) and (5)) yielded consistent results with each other. As shown in Fig. 4b, XG caused no differences in first-order kinetic constant for molecular penetration of β-LG at the air–water interface. Nevertheless, as it can be seen in Fig. 4c, the presence of XG caused a significant increment in the β-LG interfacial rearrangement rate. At long-term adsorption, this behaviour would indicate that XG in the interface vicinity could induce higher exposure rates (unfolding) and interactions (rearrangements) among the hydrophobic *patches* of unfolded protein through segregative mechanisms at the interface [44,57]. Macromolecular interactions at the air–water interface between β-LG adsorbed segments (protein–protein interactions) increased gradually and seemed to be promoted at the highest XG bulk concentration. In general, this observation was consistent with *E* values for β-LG/XG mixed systems (Fig. 2) discussed in previous sections. Thus, an increased conformational rearrangement rate of β-LG adsorbed residues at

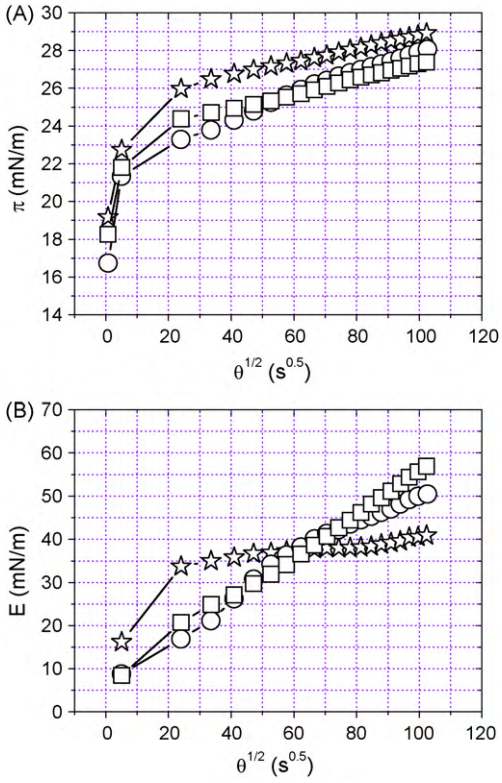

Fig. 5. Time dependence of surface pressure, π (A) and surface dilatational modulus, E (B) for (☆) WPC adsorbed films at the air–water interface as a function of XG bulk concentration (0.00–0.25 wt%). WPC:XG Symbols: (□) 1.00:0.25 wt% and (◯) 1.00:0.10 wt%. WPC concentration 1.00 wt%, temperature 20 °C, pH 7, and I 0.05 M.

air–water interface could be responsible for the greater mechanical resistance to dilatational deformation of β-LG/XG adsorbed films.

3.3. Impact of WPC/XG interaction on protein surface properties

3.3.1. Surface pressure

Dynamic surface pressure (π) for WPC adsorbed films at the air–water interface as a function of XG bulk concentration (0.00–0.25 wt%) is plotted in Fig. 5a. It was noticed that XG had a particular effect on WPC surface characteristics and consequently on the protein adsorbed film formation. Contrarily to the observed behaviour for β-LG/XG systems, XG caused a decrease in the surface pressure of WPC adsorbed film at the air–water interface (Fig. 5a). A similar phenomenon was observed in the surface pressure characteristics for WPC/λ–C and WPC/SA mixed systems [44]. In the present study, the observed behaviour could be related to WPC reduced availability for interfacial adsorption, possibly due to protein aggregation in the presence of XG in solution. However, since the tested biopolymer concentration was relatively low, phase separation in WPC/XG mixed systems was not detected.

On the other hand, in the absence of XG, π values were higher for WPC compared to β-LG adsorbed films (Fig. 2a). Although, β-LG is the majority protein fraction in WPC, this result could be associated with the presence of fat impurities [66] and other surface-active components in the sample [30]. Moreover, π values for WPC/XG mixed systems were similar to β-LG/XG systems mainly at long adsorption times (as deduced from π values for WPC/XG and β-LG/XG systems in Figs. 2a and 5a, respectively). This finding suggests that XG could promote the interfacial adsorption of β-LG present in the WPC/XG mixed systems. However, due to WPC chemical complexity, additional studies would be needed to confirm this hypothesis.

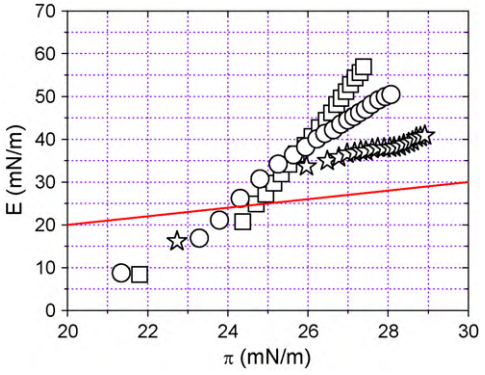

Fig. 6. Surface dilatational modulus (E) as a function of surface pressure (π) for (☆) WPC adsorbed films at the air–water interface and XG bulk concentration (0.00–0.25 wt%). WPC:XG Symbols: (□) 1.00:0.25 wt% and (◯) 1.00:0.10 wt%. WPC concentration 1.00 wt%, temperature 20 °C, pH 7, and I 0.05 M.

3.3.2. Surface dilatational properties

Dynamic dilatational modulus (E) for WPC adsorbed films at the air–water interface as a function of XG bulk concentration (0.00–0.25 wt%) is plotted in Fig. 5b. It can be observed that the WPC/XG aqueous systems showed time-dependent interfacial viscoelastic behaviour. At short adsorption time, XG caused a decrease in E values for WPC adsorbed films. This behaviour could be related to lower interactions between adsorbed protein residues, which would confirm the existence of WPC reduced availability for interfacial adsorption. However, at long-term adsorption, the magnitude of E values for the WPC adsorbed film increased with the increment of XG bulk concentration. These results suggest that macromolecular interactions between WPC adsorbed segments at the air–water interface increased gradually and seemed to be promoted at the highest XG bulk concentration. Similar results were obtained for the viscoelastic behaviour of WPC/SA and WPC/λ–C adsorbed films [44,45].

On the other hand, in the absence of XG, E values for WPC and β-LG adsorbed films were similar mainly at short adsorption times (as deduced from E values for WPC and β-LG systems in Figs. 5b and 2b, respectively). However, at long-term adsorption the E values for β-LG were higher than for WPC adsorbed films which could be associated with differences in the molecular composition of MWP samples. Protein aggregation and/or the presence of fat impurities and other surface-active molecules in the WPC sample could reduce macromolecular interactions between protein adsorbed segments at the air–water interface [11,66,67].

The E–π master curves for WPC/XG adsorbed films at 0.00–0.25 wt% XG bulk concentration are shown in Fig. 6. In this case, the slopes of E–π plots were higher than one (represented by the solid line in Fig. 6), suggesting the existence of a non-ideal behaviour governed by higher protein–protein interactions at the interface [64]. Similarly to β-LG/XG adsorbed films described above, E–π plots for WPC/XG adsorbed films were not normalized in a unique curve, indicating that the interfacial structuration was also affected by the presence of XG and the biopolymer relative concentration in solution. Nevertheless, over the whole range of surface pressures, E values for WPC and WPC/XG absorbed films were lower than those for β-LG and β-LG/XG absorbed films (Fig. 3). These results suggest that differences in MWP molecular composition and/or different MWP–XG interactions in solution could affect the adsorbed protein amount (as deduced from π values in Figs.

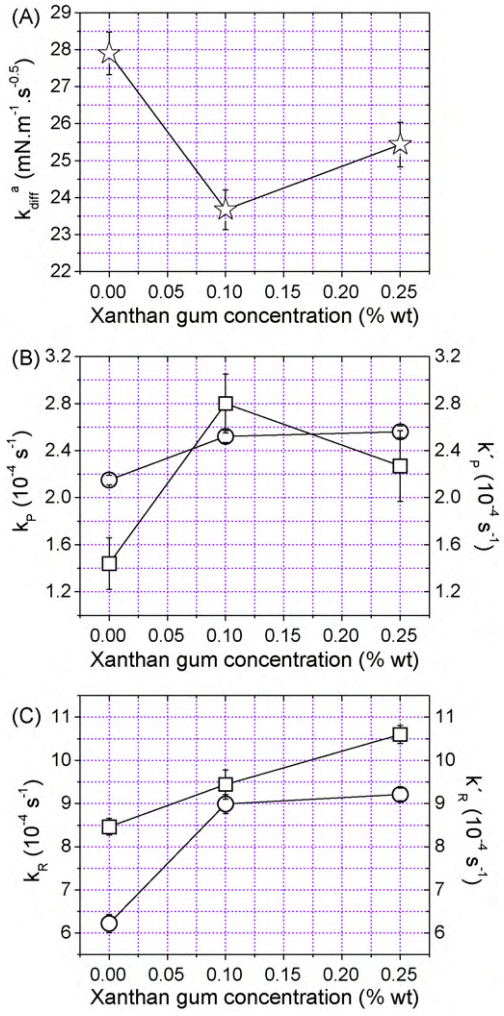

Fig. 7. Effect of XG bulk concentration (0.00–0.25 wt%) on: (A) apparent rate of diffusion to the interface (k^a_{diff}), (B) penetration rate constant obtained from Eq. (4), k_P, and Eq. (5), k'_P, and (C) configurational rearrangement rate constant obtained from Eq. (4), k_R and Eq. (5), k'_R for WPC/XG mixed systems. WPC concentration 1.00 wt%, temperature 20 °C, pH 7, and *I* 0.05 M.

2a and 5a) and protein–protein interactions at the interface (as deduced from *E* values Figs. 2b and 5b).

3.4. Impact of WPC/XG interaction on protein adsorption rheokinetics

3.4.1. Protein diffusion

Apparent diffusion rate (k^a_{diff}) for WPC as a function of XG bulk concentration (0.00–0.25 wt%) is plotted in Fig. 7a. It can be seen that XG caused a decrease in WPC diffusion rate toward the air–water interface. This behaviour may suggest that biopolymer interactions in solution of WPC/XG mixed systems could play an important role in WPC diffusion step toward the air–water interface. In order to evaluate the incidence of WPC–XG interactions in solution on the molecular diffusion behaviour toward the interface, the effect of XG bulk concentration (0.00–0.25 wt%) on WPC surface hydrophobicity (S_0) was determined [44]. S_0 values for WPC and WPC/XG mixed systems are shown in Table 1. It can be noticed that XG had an impact on the WPC S_0 values depending on its concentration in solution. In general, XG caused a decrease in WPC S_0 values which would suggest WPC aggregation in the presence of XG confirming the lowest protein diffusion toward the interface (Fig. 7a) and WPC reduced ability to form the interfacial film (as deduced from π values for WPC and WPC/XG in Fig. 5a). That is, the WPC aggregation in the presence of XG might have a significant effect on the WPC diffusion to the air–water interface and on the interfacial film formation.

On the other hand, in the absence of XG, differences in k^a_{diff} values between WPC and β-LG at the same protein concentration in solution could be attributed to differences in protein composition and/or the presence of fat impurities in the WPC sample (as deduced from k^a_{diff} values in Figs. 5a and 7a). Nevertheless, it can be seen that the WPC/XG and β-LG/XG aqueous systems showed similar values of k^a_{diff} following the same trend with the gradual increment in XG bulk concentration.

3.4.2. Protein penetration and rearrangement

Fig. 7b and c shows the application of Eqs. (4) and (5) to WPC/XG mixed systems. Differences observed among first-order kinetic constants for molecular penetration and conformational rearrangement of WPC adsorbed segments at the air–water interface could be attributed to the presence of XG and its concentration in solution. In general, it can be observed that the presence of XG in the subphase caused a significant increment in the magnitude of the first-order rate constants for the molecular penetration (Fig. 7b) and configurational rearrangement (Fig. 7c) of WPC adsorbed segments at the air–water interface.

At long-term absorption, the more aggregated state of WPC in WPC/XG mixed systems could enhance protein penetration through segregative interaction mechanisms in the vicinity of the air–water interface. Similar results were obtained for the WPC/SA mixed systems at high SA concentration in solution [44]. Moreover, in the presence of XG, the increment in WPC penetration was consistent with the increased E_v and ϕ values of the adsorbed films mainly at long adsorption times (data not shown here). This observation would indicate that the increased dilatational viscosity and relative viscoelasticity (increment in the fluid character) of WPC/XG adsorbed films could be associated with the existence of adsorbed multilayers at the interface whose formation could be promoted by the gradual increment in XG concentration [44].

Similarly to β-LG/XG mixed systems previously described, XG caused a significant increment in WPC configurational rearrangement rate (Fig. 7c). At long-term adsorption, the presence of XG in the interface vicinity could induce higher exposure rates (unfolding) and interactions (rearrangements) among WPC hydrophobic *patches* through interfacial segregative mechanisms [44,57]. This phenomenon was seemed to be promoted at the highest XG bulk concentration and it was consistent with *E* values for WPC/XG mixed systems discussed above (Fig. 5b).

On the other hand, in the absence of XG, values of the first-order rate constants for molecular penetration and configurational rearrangement for WPC were lower than those for β-LG, although the value of WPC k^a_{diff} was higher than the β-LG one (as deduced from rheokinetic constants in Figs. 4 and 7). This observation could also be attributed to differences in molecular composition [41,42] and/or to differences in protein aggregation at the air–water interface.

4. Conclusions

Macromolecular interactions between MWP and XG both in solution and at the interface vicinity depended on the protein type (β-LG or WPC) and on the biopolymer relative concentration in aqueous subphase. The main interaction mechanism that would govern MWP adsorption behaviour in MWP/XG mixed systems could be biopolymer interfacial segregation due to thermodynamic incompatibility between the MWP and XG in the vicinity of the air–water interface.

Biopolymer interfacial segregation has a significant effect on the MWP adsorption rheokinetics at the air–water interface, which has been evaluated in terms of the following mechanisms: (i) protein diffusion from the aqueous subphase toward the interface (k^{a}_{diff}), (ii) adsorption, penetration, and interfacial unfolding (k_P), and (iii) aggregation, rearrangement within the interfacial layer, multilayer formation and even interfacial gelation (k_R).

For β-LG/XG mixed systems, it can be seen that: (i) at short-term adsorption, β-LG k^{a}_{diff} increased in the presence of XG probably due to an enhanced β-LG S_0, (ii) at long-term adsorption, β-LG k_P was not altered and β-LG k_R increased in XG presence, and (iii) viscoelastic characteristics of β-LG/XG adsorbed films also depend on XG concentration in solution and on adsorption time. At short adsorption time, β-LG–XG segregative interactions in the interface vicinity could increase surface dilatational resistance, while at long-term adsorption, mechanical resistance of β-LG adsorbed films could only be improved at the highest XG concentration.

On the other hand, although WPC chemical complexity could make more difficult the comprehension of WPC interfacial behaviour from a molecular point of view, we might propose a possible interpretation for WPC/XG systems adsorption based on experimental data and previous studies. Thus, for WPC/XG mixed systems, it can be observed that: (i) at short-term adsorption, WPC k^{a}_{diff} decreased in XG presence probably due to a reduced WPC S_0 (aggregation due to XG presence in the subphase), (ii) at long-term adsorption, WPC k_P and k_R increased in the presence of XG probably due to the adsorbed multilayer formation, and (iii) viscoelastic characteristics of WPC/XG adsorbed films depended on XG concentration in solution and on adsorption time. At short-term adsorption, the poor mechanical resistance of WPC adsorbed films could be related to the reduced protein availability for the interfacial adsorption; while at long-term adsorption, the mechanical resistance of WPC adsorbed films could be improved with the increment in XG concentration.

The results obtained in the present study confirm the hypothesis that the surface dynamic properties of MWP adsorbed films could be improved by macromolecular interactions between MWP and XG. The improvement of MWP interfacial functionality derived from a rational control of MWP–XG interactions both in aqueous solution and at the air–water interface. On the basis of this information, we would attempt in a future paper to correlate the MWP interfacial rheology with MWP foam formation and stability characteristics in relation to the presence of XG in aqueous solution.

Acknowledgements

We acknowledge the financial support of the following projects: 105PI0274 (CYTED), CAI+D tipo II PI 57-283 (UNL, Santa Fe, Argentina), PICTO 36237 (ANPCyT-UNL, Argentina), PICTO 35831 (ANPCyT-UNL, Argentina), AGL2007-60045 (CICYT, US, Sevilla, Spain) and PO6-AGR-01535 (Junta de Andalucía, Spain). Authors would like to thank the Consejo Nacional de Investigaciones Científicas y Técnicas de la República Argentina (CONICET) for the postgraduate fellowship awarded to Adrián A. Perez.

References

[1] J.M. Rodríguez Patino, C. Carrera, M.R. Rodríguez Niño, Adv. Colloid Interface Sci. 140 (2008) 95.
[2] J.M. Rodríguez Patino, M.R. Rodríguez Niño, C. Carrera, Curr. Opin. Colloid Interface Sci. 12 (2007) 187.
[3] D.G. Dalgleish, Trends Food Sci. Technol. 8 (1997) 1.
[4] C. Carrera, J.M. Rodríguez Patino, Food Hydrocolloids 19 (2005) 407.
[5] K.G. Marinova, E.S. Basheva, B. Nenova, M. Temelska, A.Y. Mirarefi, B. Campbell, I.B. Ivanov, Food Hydrocolloids 23 (2009) 1864.
[6] F. MacRitchie, Adv. Protein Chem. 32 (1978) 283.
[7] E. Tornberg, J. Colloid Interface Sci. 64 (1978) 391.
[8] D.E. Graham, M.C. Phillips, J. Colloid Interface Sci. 70 (1979) 403.
[9] S. Damodaran, K.B. Song, Biochim. Biophys. Acta 954 (1988) 253.
[10] E. Dickinson, Colloids Surf. B: Biointerfaces 15 (1999) 161.
[11] A. Mackie, P. Wilde, Adv. Colloid Interface Sci. 117 (2005) 3.
[12] B.S. Murray, Curr. Opin. Colloid Interface Sci. 7 (2002) 426.
[13] V.B. Tolstoguzov, Food Hydrocolloids 17 (2003) 1.
[14] E. Dickinson, Colloids Surf. A: Phys. Eng. Aspects 288 (2006) 3.
[15] H. Schubert, K. Ax, O. Behrend, Trends Food Sci. Technol. 14 (2003) 9.
[16] A. Moure, J. Sineiro, H. Dominguez, J.C. Parajó, Food Res. Int. 39 (2006) 945.
[17] C. Balerin, P. Aymard, F. Ducept, S. Vaslin, G. Cuvelier, J. Food Eng. 78 (2007) 802.
[18] J.J. Bimbenet, H. Schubert, G. Trystram, J. Food Eng. 78 (2007) 390.
[19] I. Narchi, Ch. Vial, G. Djelveh, Food Hydrocolloids 23 (2009) 188.
[20] A. Saxena, B.P. Tripathi, M. Kumar, V.K. Shahi, Adv. Colloid Interface Sci. 145 (2009) 1.
[21] L. He, A.F. Dexter, A.P.J. Middelberg, Chem. Eng. Sci. 61 (2006) 989.
[22] J.M. Rodríguez Patino, A. Lucero Caro, M.R. Rodríguez Niño, A.R. Mackie, A.P. Gunning, V.J. Morris, Food Chem. 102 (2007) 532.
[23] E. Dickinson, Food Hydrocolloids 23 (2009) 1473.
[24] L.G. Phillips, W. Schulman, J.E. Kinsella, J. Food Sci. 55 (1990) 1116.
[25] K. Demetriades, J.N. Coupland, D.J. McClements, J. Food Sci. 62 (1997) 462.
[26] J.P. Davis, E.A. Foegeding, F.K. Hansen, Colloids Surf. B: Biointerfaces 34 (2004) 13–23.
[27] J.M. Álvarez Gómez, V.M. Pizones Ruíz-H, C. Carrera, J.M. Rodríguez Patino, Food Hydrocolloids 22 (2008) 1105.
[28] D. Guzey, D.J. McClements, J. Weiss, Food Res. Int. 36 (2003) 649.
[29] X. Yang, T.K. Berry, E.A. Foegeding, J. Food Sci. 74 (2009) 259.
[30] M.J. Martinez, C. Carrera, J.M. Rodríguez Patino, A.M.R. Pilosof, Colloids Surf. B: Biointerfaces 68 (2009) 39.
[31] R.I. Baeza, C. Carrera, A.M.R. Pilosof, J.M. Rodríguez Patino, Food Hydrocolloids 19 (2005) 239.
[32] R.A. Ganzevles, M.A. Cohen Stuart, T. van Vliet, H.H.J. de Jongh, Food Hydrocolloids 20 (2006) 872.
[33] R.I. Baeza, C. Carrera, A.M.R. Pilosof, J.M. Rodríguez Patino, AIChE J. 52 (2006) 2627.
[34] R.A. Ganzevles, K. Zinoviadou, T. van Vliet, M.A. Cohen Stuart, H.H.J. de Jongh, Langmuir 22 (2006) 10089.
[35] B.T. Stokke, A. Elgsaeter, G. Skjak-Braek, O. Smidsrod, Carbohydr. Res. 160 (1987) 13.
[36] E.A. Foegeding, J.P. Davis, D. Doucet, M.K. McGuffey, Trends Food Sci. Technol. 13 (2002) 151.
[37] T.K. Berry, X. Yang, E.A. Foegeding, J. Food Sci. 74 (2009) 269.
[38] M.E. Mangino, Y.Y. Liao, N.J. Harper, C.V. Morr, J.G. Zadow, J. Food Sci. 52 (1987) 1522.
[39] W.L. Hurley, B.L. Ventling, M. Ma, B.L. Larson, J. Food Qual. 13 (1990) 119.
[40] T. Wang, L.A. Lucey, J. Dairy Sci. 86 (2003) 3090.
[41] H. Zhu, S. Damodaran, J. Food Sci. 59 (1994) 554.
[42] M.N. Vaghela, A. Kilara, J. Food Sci. 61 (1996) 275.
[43] L.M. Huffman, J.M. Harper, J. Dairy Sci. 82 (1999) 2238.
[44] A.A. Perez, C.R. Carrara, C. Carrera, L.G. Santiago, J.M. Rodríguez Patino, Food Hydrocolloids 23 (2009) 1253.
[45] A.A. Perez, C.R. Carrara, C. Carrera, L.G. Santiago, J.M. Rodríguez Patino, AIChE J. 56 (2009) 1107.
[46] A.A. Perez, C.R. Carrara, C. Carrera, J.M. Rodríguez Patino, L.G. Santiago, Food Chem. 116 (2009) 104.
[47] AACC Methods of American Association of Cereal Chemists (1983) Method 46-23.
[48] J.N. de Wit, E. Hontelez-Backx, M. Adamse, Neth. Milk Dairy J. 42 (1988) 155.
[49] A. Kato, S. Nakai, Biochim. Biophys. Acta 624 (1980) 13.
[50] C. Carrera, M.R. Rodríguez Niño, A. Lucero Caro, J.M. Rodríguez Patino, J. Food Eng. 67 (2005) 225.
[51] J.M. Rodríguez Patino, M.R. Rodríguez Niño, C. Carrera, J. Agric. Food Chem. 47 (1999) 2241.
[52] J. Lucassen, M. van den Tempel, Chem. Eng. Sci. 27 (1972) 1283.
[53] A.F.H. Ward, L. Tordai, J. Chem. Phys. 14 (1946) 353.
[54] S. Xu, S. Damodaran, Langmuir 10 (1994) 472.
[55] F. MacRitchie, A.E. Alexander, J. Colloid Interface Sci. 18 (1963) 458.
[56] D.E. Graham, M.C. Phillips, J. Colloid Interface Sci. 70 (1979) 427.
[57] G.E. Pavlovskaya, M.G. Semenova, E.N. Thzapkina, V.B. Tolstoguzov, Food Hydrocolloids 7 (1993) 1.
[58] Y. Cao, S. Damodaran, J. Agric. Food Chem. 43 (1995) 2567.
[59] L. Razumovsky, S. Damodaran, J. Agric. Food Chem. 49 (2001) 3080.
[60] T. Sengupta, S. Damodaran, J. Agric. Food Chem. 49 (2001) 3087.
[61] S. Damodaran, L. Razumovsky, Food Hydrocolloids 17 (2003) 355.
[62] J.M. Rodríguez Patino, C. Carrera, M.R. Rodríguez Niño, M. Cejudo, J. Colloid Interface Sci. 242 (1999) 141.
[63] J.M. Rodríguez Patino, S.E. Molina, C. Carrera, M.R. Rodríguez Niño, M.C. Añón, J. Colloid Interface Sci. 268 (2003) 50.
[64] E.H. Lucassen Reynders, J. Lucassen, P.R. Garrett, D. Giles, F. Hollway, Adv. Chem. Ser. 144 (1975) 272.
[65] J.M. Rodríguez Patino, C. Carrera, S.E. Molina, M.R. Rodríguez Niño, M.C. Añón, Ind. Eng. Chem. Res. 43 (2004) 1681.
[66] M. Cornec, G. Narsimhan, J. Agric. Food Chem. 46 (1998) 2490.
[67] J.M. Rodríguez Patino, M.R. Rodríguez Niño, C. Carrera, Curr. Opin. Colloid Interface Sci. 8 (2003) 387.